J|A|C|S
ARTICLES
Published on Web 02/02/2006

Protein Ligand Design: From Phage Display to Synthetic Protein Epitope Mimetics in Human Antibody Fc-Binding Peptidomimetics

Ricardo L. A. Dias,[†] Rudi Fasan,[†] Kerstin Moehle,[†] Annabelle Renard,[†] Daniel Obrecht,[‡] and John A. Robinson*,[†]

Contribution from the Institute of Organic Chemistry, University of Zurich, Winterthurerstrasse 190, 8057-Zurich, and Polyphor AG, 4123-Allschwil, Switzerland

Received November 3, 2005; E-mail: robinson@oci.unizh.ch

Abstract: Phage display is a powerful method for selecting peptides with novel binding functions. Synthetic peptidomimetic chemistry is a powerful tool for creating structural diversity in ligands as a means to establish structure−activity relationships. Here we illustrate a method of bridging these two methodologies, by starting with a disulfide bridged phage display peptide which binds a human antibody Fc fragment (Delano et al. *Science* **2000**, *287*, 1279) and creating a backbone cyclic β-hairpin peptidomimetic with 80-fold higher affinity for the Fc domain. The peptidomimetic is shown to adopt a well-defined β-hairpin conformation in aqueous solution, with a bulge in one β-strand, as seen in the crystal structure of the phage peptide bound to the Fc domain. The higher binding affinity of the peptidomimetic presumably reflects the effect of constraining the free ligand into the conformation required for binding, thus highlighting in this example the influence that ligand flexibility has on the binding energy. Since phage display peptides against a wide variety of different proteins are now accessible, this approach to synthetic ligand design might be applied to many other medicinally and biotechnologically interesting target proteins.

Introduction

Phage display is a well-established technology for selecting peptides and proteins with novel binding functions.[1] Since the method involves fusing libraries of DNA fragments to genes encoding bacteriophage coat proteins, such that the fusion genes are encapsulated within viable phage particles and the phages also display the encoded peptides on their surface, a physical link is established between the binding properties of individual phage and their genetic sequence. One of the reasons why phage display technology is so successful is that very large peptide libraries (over 10^9) can, in principle, be produced and screened. From the viewpoint of introducing structural diversity, however, a limitation is that the peptides displayed on phage particles are built using proteinogenic amino acids linked through peptide bonds. In contrast, peptidomimetic chemistry can draw on the resources of synthesis to introduce enormous structural variety into potential protein ligands, although a limitation is that only very modest library sizes can then be achieved when the goal is to produce pure compounds for screening purposes by parallel combinatorial synthesis. It is, therefore, interesting to explore ways of linking these two methodologies, such that the advantages of both can be harnessed for ligand discovery and optimization.[2,3]

In this work, we describe an approach to elaborate disulfide-bridged peptides from phage display using protein epitope mimetic technology. Protein epitope mimetics (PEMs) as described here are backbone cyclic peptidomimetics that incorporate a template moiety to stabilize an attached loop in a β-hairpin conformation. A restrained β-hairpin backbone can be used as a scaffold to display and position the energetically important groups needed for protein (receptor) recognition. We have shown in earlier work that β-hairpin PEMs containing a D-Pro-L-Pro template can be synthesized using combinatorial, parallel synthesis approaches and that their size, β-hairpin conformation, and biological activity can be optimized by the appropriate choice of building blocks.[4−12]

[†] University of Zurich.
[‡] Polyphor AG.

(1) Sidhu, S. S.; Fairbrother, W. J.; Deshayes, K. *ChemBioChem* **2003**, *4*, 14−25.
(2) Dwyer, M. A.; Lu, W.; Dwyer, J. J.; Kossiakoff, A. A. *Chem. Biol.* **2000**, *7*, 263−274.
(3) Rutledge, S. E.; Volkman, H. M.; Schepartz, A. *J. Am. Chem. Soc.* **2003**, *125*, 14336−14347.
(4) Späth, J.; Stuart, F.; Jiang, L.; Robinson, J. A. *Helv. Chim. Acta* **1998**, *9*, 1726−1738.
(5) Jiang, L.; Moehle, K.; Dhanapal, B.; Obrecht, D.; Robinson, J. A. *Helv. Chim. Acta* **2000**, *83*, 3097−3112.
(6) Favre, M.; Moehle, K.; Jiang, L.; Pfeiffer, B.; Robinson, J. A. *J. Am. Chem. Soc.* **1999**, *121*, 2679−2685.
(7) Fasan, R.; Dias, R. L. A.; Moehle, K.; Zerbe, O.; Vrijbloed, J. W.; Obrecht, D.; Robinson, J. A. *Angew. Chem., Int. Ed.* **2004**, *43*, 2109−2112.
(8) Descours, A.; Moehle, K.; Renard, A.; Robinson, J. A. *ChemBioChem* **2002**, *3*, 318−323.
(9) Shankaramma, S. C.; Athanassiou, Z.; Zerbe, O.; Moehle, K.; Mouton, C.; Bernardini, F.; Vrijbloed, J. W.; Obrecht, D.; Robinson, J. A. *ChemBioChem* **2002**, *3*, 1126−1133.
(10) Shankaramma, S. C.; Moehle, K.; James, S.; Vrijbloed, J. W.; Obrecht, D.; Robinson, J. A. *Chem. Commun.* **2003**, 1842−1843.
(11) Robinson, J. A.; Shankaramma, S. C.; Jetter, P.; Kienzl, U.; Schwendener, R. A.; Vrijbloed, J. W.; Obrecht, D. *Bioorg. Med. Chem.* **2005**, *13*, 2055−2064.
(12) Athanassiou, Z.; Dias, R. L. A.; Moehle, K.; Dobson, N.; Varani, G.; Robinson, J. A. *J. Am. Chem. Soc.* **2004**, *126*, 6906−6913.

10.1021/ja057513w CCC: $33.50

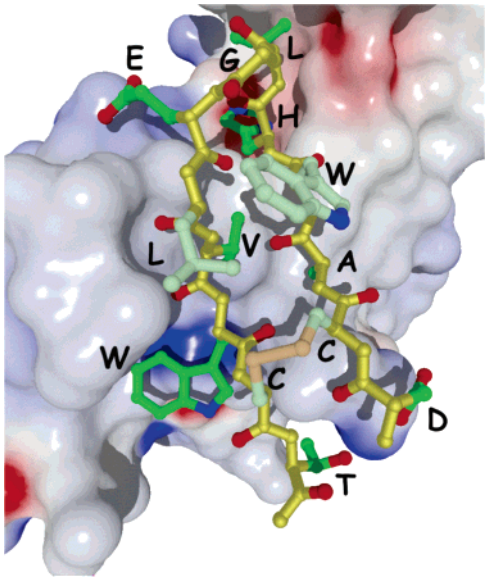

Figure 1. Fc-III peptide (DCAWHLGELVWCT) as a stick model bound to the surface of the Fc domain (PDB file 1DN2).[13] The Fc-III backbone is yellow (O atoms red), side chains making contact with Fc are dark green, those pointing toward solvent are light green, and the disulfide bridge is brown.

Here we focus on a phage display peptide (Fc-III), which was selected by panning against a human monoclonal antibody Fc domain.[13] This disulfide bridged peptide binds the Fc and inhibits binding of Protein A (Z-domain) with an apparent K_i of 25 nM (by competition ELISA), which is only about 2-fold weaker than the affinities of Protein A and Protein G ($K_D \approx 10$ nM) for Fc. A crystal structure of the Fc-III peptide in complex with Fc at 2.7 Å resolution[13] showed the peptide constrained into a β-hairpin conformation by the disulfide bridge and bound to the consensus binding site recognized by several natural Fc-binding proteins, including Protein A. A peptide constrained by a single disulfide bridge, however, is not an optimal starting point for many synthetic operations due to its reactivity. Moreover a single disulfide bridge may provide only a limited conformational restriction. Indeed, the conformation of the Fc-III peptide free in solution has not been described.[13] On the other hand, a backbone cyclic peptide provides an excellent scaffold for synthetic modification, and the introduction of a structure-inducing template as well as other cross-links provides a means to tailor the conformation of the molecule for the target receptor. Here we show that, by grafting the Fc-III peptide loop onto a hairpin-inducing D-Pro-L-Pro template, backbone cyclic synthetic PEMs can be produced having a significantly higher affinity for the human Fc fragment. Moreover, the way is then opened for further modification and tuning of the physical and biological properties of the mimetics using synthesis.

Results

Design and Synthesis of Mimetics. The backbone conformation of the phage-derived Fc-III peptide (DCAWHLGELVWCT-NH_2) in the complex with Fc (PDB file 1DN2) was the starting point for mimetic design (Figure 1). Computer models of two PEMs were generated by transposing residues Ala3-Trp11, or residues Asp1-Thr13, from bound Fc-III, onto a D-Pro-L-Pro template, to afford FcBP-1 and FcBP-2, respectively (Figure 2). The conformation of the D-Pro-L-Pro template was taken from the crystal structure of Pivaloyl-D-Pro-L-Pro-L-Ala-NHMe.[14] After transposition and geometry optimization, the bond vectors of the carbonyl groups attached to the pyrrolidine rings of the template, as well as the ϕ/ψ values of residues around the loop, remain essentially unaltered.

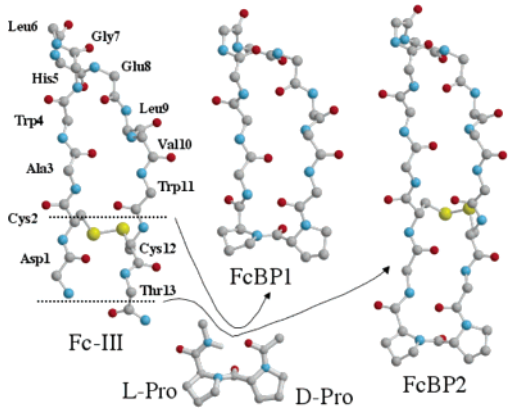

Figure 2. Computer models of FcBP-1 and FcBP-2 made by transplanting 9 or 13 residues, respectively, from Fc-III onto the D-Pro-L-Pro template. The directional register of carbonyl groups in each β-strand in Fc-III should be maintained upon transplanting the loops to the template.

The two mimetics, FcBP-1 and FcBP-2, were synthesized by a strategy involving solid-phase peptide assembly using Fmoc-chemistry and a solution-phase macrocyclization, in analogy to earlier work.[5] After side chain deprotection, FcBP-1 was purified directly by HPLC, whereas for FcBP-2 the dithiol form was air-oxidized to install the disulfide bridge and then purified. Both mimetics were characterized by MS and NMR (see Supporting Information).

Fc-Protein A Inhibition Assay. A BIAcore instrument was used to quantify inhibition of human monoclonal IgG_1 (herceptin) binding to an engineered Z domain based on staphylococcal Protein A.[15] The Z-domain was produced in *E. coli* as a fusion protein with glutathione S-methyl transferase (GST). The GST-Z fusion protein was coupled to the surface of a CM5 sensor chip (BIACORE, AB) by random amine coupling. A reference surface was prepared by coupling the same amount of GST in a separate flow cell. Then human monoclonal IgG_1 (25 nM) was incubated with various concentrations of peptide or mimetic at pH 7.4, before injection over the test and reference sensor surfaces (Figure 3). Using the responses, IC_{50} values could be determined (Table 1) for the phage-derived peptide Fc-III, the two mimetics FcBP-1 and Fc-BP2, and, for comparison, Protein A, the GST-Z fusion protein, and recombinant isolated Z domain, as well as the reduced dithiol derivatives of Fc-III and FcBP-2 (i.e., with the disulfide bridge cleaved).

Protein A shows an IC_{50} of 3.3 nM, a 10-fold lower value than GST-Z fusion protein. Compared to these Fc-binding proteins, the 13-mer peptide Fc-III shows a considerably lower affinity for the IgG_1 ($IC_{50} = 460$ nM), and a complete loss of affinity is observed when the disulfide bridge is reduced. Compared to Fc-III, FcBP-1 binds the Fc fragment with a much

(13) DeLano, W. L.; Ultsch, M. H.; de Vos, A. M.; Wells, J. A. *Science* **2000**, *287*, 1279−1283.
(14) Nair, C. M.; Vijayan, M.; Venkatachalapathi, Y. V.; Balaram, P. *J. Chem. Soc., Chem. Commun.* **1979**, 1183−1184.
(15) Nilsson, B.; Moks, T.; Jansson, B.; Abrahmsén, L.; Elmblad, A.; Holmgren, E.; Henrichson, C.; Jones, T. A.; Uhlén, M. *Protein Engineering* **1987**, *1*, 107−113.

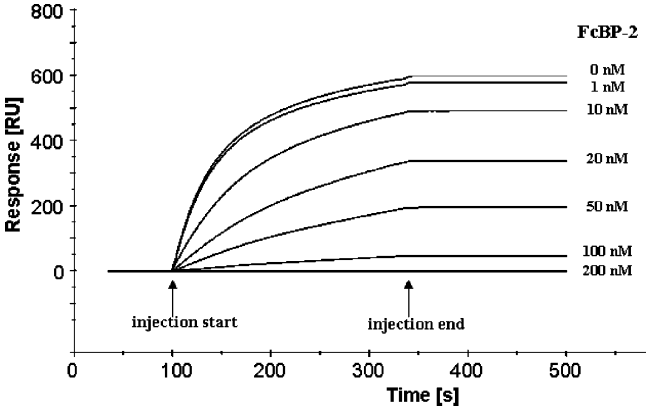

Figure 3. Sensorgrams from a BIAcore inhibition assay with GST-Z-domain fusion protein immobilized on the sensor surface, and human IgG_1 and increasing concentrations of inhibitor (FcBP-2) in solution. The response vs peptide concentration was used to determine IC_{50} values.

Table 1. Affinities of Various Ligands for the Fc Domain[a]

ligand	IC_{50} (nM)	K_i (nM)
Protein A	3.3 ± 0.3	nd
GST-Z-domain	37 ± 7.1	nd
Z-domain	53 ± 2.8	nd
Fc-III, pH 7.4	460 ± 74	215
Fc-III, pH 6.0	280 ± 41	41
Fc-III reduced	$>10^6$	nd
FcBP-1, pH 7.4	$64\,800 \pm 4400$	14 200
FcBP-1, pH 6.0	395000 ± 7100	71 000
FcBP-2, pH 7.4	32 ± 2	0.4
FcBP-2, pH 6.0	35 ± 2	2.0
FcBP-2red, pH 7.4	550 ± 50	nd

[a] IC_{50} values are from competition BIAcore assays (see Figure 3) with standard deviations from at least three independent experiments. K_i values were determined by the method described by DeLano et al.[13] (see text). nd = not determined.

lower affinity ($IC_{50} \approx 65\ \mu M$). However, FcBP-2 shows a significant improvement in binding affinity ($IC_{50} = 32$ nM), which is higher even than that of the Z domain. Upon reduction of the intramolecular disulfide bond in FcBP-2, a significant part of the Fc-binding affinity is retained ($IC_{50} = 550$ nM).

Control experiments were performed employing an IgG_1 from a different species (mouse monoclonal anti-c-Myc antibody 9E10) and testing the inhibitory potency of an unrelated peptide (*cyclo*(PFLWLNKETp)). In both cases no inhibition was observed, confirming the specificity of the interaction between the human IgG_1 and the mimetics.

Influence of pH and Direct Affinity Measurements. The Fc-III peptide was reported to inhibit the Protein A (Z domain)−Fc interaction 4-fold more tightly at pH 6.0 than at pH 7.2. The influence of pH on the affinities of FcBP-1 and -2 for the Fc was therefore examined. To facilitate a comparison with the reported binding activity of Fc-III, binding constants were determined following the published method[13] by extrapolating IC_{50} values measured at various Fc concentrations to zero to obtain K_i (Table 1). However, it should be noted that not only the assay conditions but also the Fc-containing proteins used are different, so the absolute affinities will not be directly comparable to those of DeLano et al.[13] However, the trends in binding affinities are reproduced. Thus, Fc-III shows improved binding to Fc at pH 6.0 compared to pH 7.4, in good agreement with the results of DeLano et al.[13] FcBP-1 shows a reverse behavior, with higher affinity at pH 7.4 than at 6.0. In contrast, FcBP-2 shows no pH effect, with the affinity essentially the same at pH 7.4 and 6.0.

Table 2. Dissociation Constants (K_D) and k_{on} and k_{off} for Fc-III and FcBP-2 Determined by Direct BIAcore

	K_D (nM)	k_{on} [$M^{-1}\,s^{-1}$]	k_{off} [s^{-1}]
		Fc-III	
pH 7.4	185	$(3.75 \pm 0.62) \times 10^5$	$(6.96 \pm 1.66) \times 10^{-2}$
pH 6.0	125	$(2.48 \pm 0.18) \times 10^5$	$(3.12 \pm 0.71) \times 10^{-2}$
		FcBP-2	
pH 7.4	2.2	$(4.83 \pm 0.86) \times 10^6$	$(1.07 \pm 0.07) \times 10^{-2}$
pH 6.0	1.8	$(7.43 \pm 0.35) \times 10^6$	$(1.37 \pm 0.13) \times 10^{-2}$

The affinities (K_d) of Fc-III and FcBP-2 for the Fc domain were also measured directly using a BIAcore 3000 system and a sensor chip surface prepared by immobilizing the human monoclonal IgG_1. Upon introducing the ligands, the binding reactions with Fc-III, FcBP-1, and FcBP-2 gave response curves (see Supporting Information) that could be fitted to a binding equation describing a 1:1 interaction. The excellent quality of the fit is indicated by the small and random distribution of residuals, the low χ^2 (<0.5 RU) and the small standard errors for the estimates of k_{on}, k_{off}, and R_{max}. The derived K_D's show that the mimetic FcBP-2 has an ~80-fold higher affinity for the Fc domain at pH 7.4 than does Fc-III (Table 2). The binding affinity of FcBP-2 is also essentially independent of pH in the range measured.

Conformational Studies by NMR. The conformations of the mimetics were investigated by NMR spectroscopy, FcBP-1 in water−methanol (1:3) solution pH 6.0, and FcBP-2 in aqueous solution pH 6.0. Chemical shift assignments were achieved by standard methods. It was not possible to study Fc-III under comparable conditions due to its poor solubility.

FcBP-1. This mimetic showed two sets of ^1H resonances in a ca. 1:2 ratio in the range pH 2−5, but this ratio changed to ca. 1:10 upon raising the pH from 5.0 to 6.0 and remained unchanged to pH 7.0. The assignments for the major form are reported in the Supporting Information. Peak overlap prevented a complete assignment of the NMR spectrum of the minor form. Analysis of ROEs in ROESY plots provided strong prima facia evidence for a well-defined backbone conformation in the major form of the mimetic but not the one expected. A full list of ROE connectivities are provided in the Supporting Information.

Notable ROEs are the $d_{\alpha\alpha}$ (i,i+1) and (i,i+2) connectivities seen within the four residues Trp9-^{D}Pro10-^{L}Pro12-Ala1, including strong $d_{\alpha\alpha}(i,i+1)$ ROEs between both ^{D}Pro10 and ^{L}Pro11 and Trp9 and ^{D}Pro10, as well as a $d_{\alpha\alpha}(i,i+2)$ ROE between Trp9 and ^{L}Pro11 (Figures 4 and 5). These ROEs indicate the presence of a tight turn conformation and demonstrate also, remarkably, the presence of two consecutive *cis* peptide bonds, one between Trp9 and ^{D}Pro10 and another linking ^{D}Pro10 and ^{L}Pro11.

Furthermore, a strong $d_{\alpha\alpha}(i,i+5)$ ROE is seen (Figure 5) between Trp2 and Leu7. This ROE is not characteristic of the expected β-hairpin conformation, which would require Trp2 C(α)−H to be in close proximity to Val8 C(α)−H and not Leu7 C(α)−H. Nevertheless, the considerable number of long-range ROEs seen between Trp2 and Leu7/Glu6, and between His3 and Val8, provide support for a well defined conformation in this mimetic. The minor conformer detected by NMR appears to contain all-*trans* peptide bonds, since characteristic ROEs between Trp9 C(α)−H and ^{D}Pro10 C(δ)−H and between

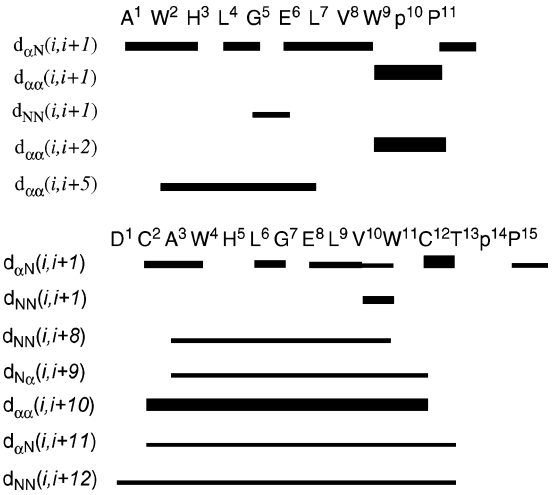

Figure 4. Summary of ROE connectivities along the backbone of FcBP-1 (top) and FcBP-2 (bottom) detected in ROESY spectra. Thick, medium, thin bars = strong, medium, weak ROEs, respectively.

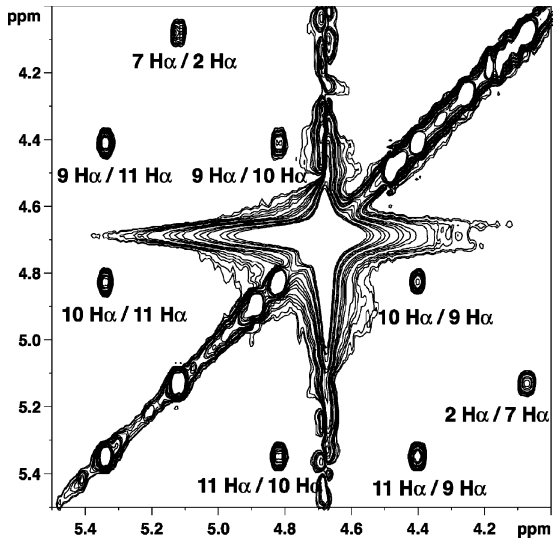

Figure 5. Part of a 600 MHz ^{1}H ROESY spectrum of FcBP-1. Cross-peaks due to four C(α)−H to C(α)−H ROE connectivities are shown (see text), including three indicative of the double *cis* peptide bonds between Trp9 and ^{D}Pro10 and between ^{D}Pro10 and ^{L}Pro11.

^{D}Pro10 C(α)−H and ^{L}Pro11 C(*δ*)−H were observed. However, peak overlap prevented a full analysis of the solution conformation of this minor form.

Average solution structures were calculated for the major form of FcBP-1 using the available ROE-derived distance restraints. The resulting structures were geometry optimized by MD, and results are reported in Table 3. The average solution structures converge to a family of closely related backbone conformers (Figure 6). All the structures contain two consecutive *cis*-peptide bonds between Trp9 and ^{D}Pro10 and between ^{D}-Pro10 and ^{L}Pro11. The loop backbone has a distorted hairpin conformation with a three-residue *γ*-turn defined by residues His3-Leu4-Gly5. The backbone conformation of FcBP-1 is similar to that of bound Fc-III (Figure 7A), and most side chains of FcBP-1 adopt similar positions with respect to the plane of the hairpin, with the exception of the FcBP-1 Trp9 side chain (Figure 7B). This is oriented on the opposite (i.e., wrong) face of the hairpin compared to the corresponding Trp11 side chain in Fc-III. The side chains of Trp2, Leu7, and Trp9 in FcBP-1

Table 3. Summary of the Upper Distance Restraints, the Residual Target Functions of the Final 20 DYANA Structures, the rmsd Values upon Superimposition, and Residual Restraint Violations for Structure Calculations of FcBP-1 and FcBP-2

	FcBP-1	FcBP-2
NOE upper-distance limits	87	107
intraresidue	29	30
sequential	31	42
medium- and longe-range	27	35
residual target function (Å^2)	1.28 ± 0.07	0.45 ± 0.02
mean rmsd values (Å)		
all backbone atoms	0.77 ± 0.26	0.80 ± 0.25
all heavy atoms	1.33 ± 0.35	1.42 ± 0.29
residual NOE violation		
number > 0.2 Å	6	1
maximum (Å)	0.30	0.21

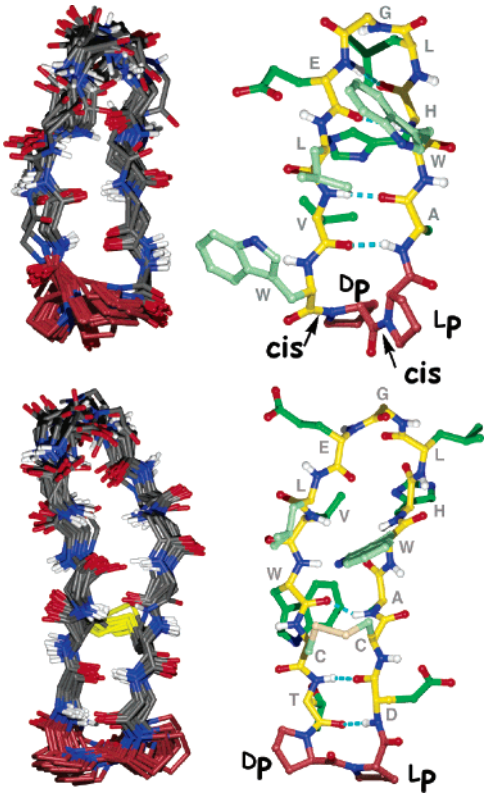

Figure 6. Superimposition of the final 20 NMR structures for FcBP-1 (top) and FcBP-2 (bottom). The template residues (^{D}Pro-^{L}Pro) are at the bottom in brown. One representative structure is shown for each mimetic. Note the two *cis* peptide bonds in FcBP-1. Yellow = backbone carbons, red = O atoms, blue = N atoms, light green = side chains pointing up, dark green = side chains pointing down (see also Figures 1 and 7).

form a hydrophobic cluster on one side of the loop, with Leu7 sandwiched between the two aromatic rings of Trp2 and Trp9. This stacking interaction nicely explains one feature of the ^{1}H NMR spectrum of FcBP-1, namely the high field shifted resonances (−0.04, +0.45 ppm) of the methyl groups in the Leu7 side chain.

FcBP-2. This mimetic shows a single set of ^{1}H NMR resonances in aqueous solution. The assignments and ROE distance restraints are given in the Supporting Information. The observed ROE connectivities show that all peptide bonds are *trans* and that the template forms, as expected (Figure 2), a type-II′ *β*-turn. A strong NOE is seen between the C(α)−H protons of Cys2 and Cys12, consistent with the expected *β*-hairpin backbone conformation. This conclusion is strength-

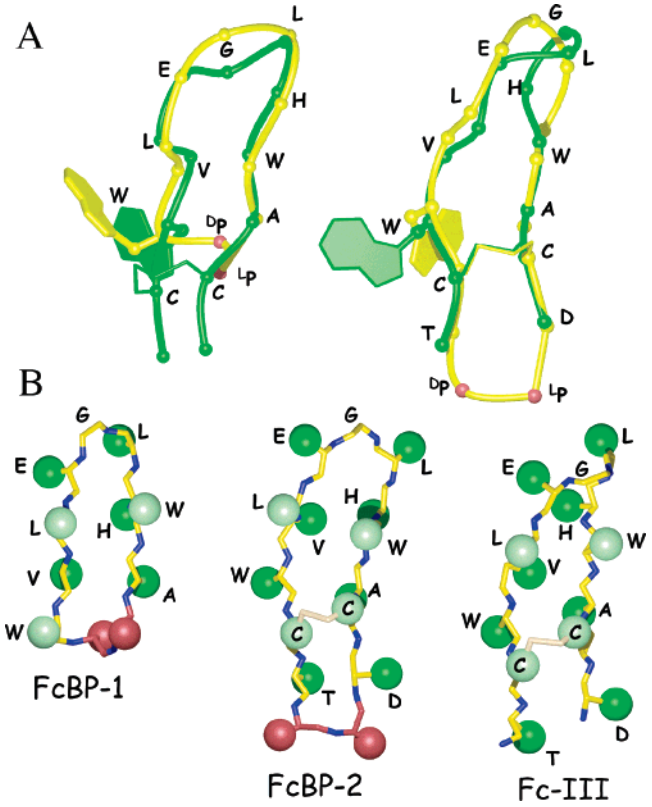

Figure 7. (A) Superimposition over the backbone atoms of the bound structure of Fc-III (green) with representative NMR structures of FcBP-1 and FcBP-2 (yellow). The ribbon traces the backbone, and the balls represent the C(α) atoms. (B) The backbone of each peptide is shown alone (C atoms, yellow; N atoms, blue) as well as the C(β) atom of each side chain is shown as a large ball. The side chains pointing up = light green, the side chains pointing down = dark green (compare Figure 1). Template residues are brown.

ened by numerous long-range NOEs from main chain and side chain interactions between residues on opposite sides of the hairpin (Asp1/Cys2/Ala3/Trp4 connectivities with Leu9/Val10/Trp11/Cys12/Thr13) (see Figure 4 and Supporting Information). The network of observed NOEs is very characteristic of an antiparallel arrangement of the two adjacent β-strands. However, there is a strong sequential HN−HN NOE betwen Val10 and Trp11, which would not occur in a regular β-structure, and is indicative here of a bulge in the second β-strand at Val10. Only a few sequential NOEs were observed in the tip region His5/Leu6/Gly7/Glu8 indicating that this part of the molecule could be more flexible in solution.

Average solution structures were calculated for FcBP-2. The ensemble of resulting structures contains closely related β-hairpin conformations, with no significant distance restraint violations (Figure 6 and Table 3). The peptide backbone is characterized by a high degree of apparent conformational rigidity, especially in the region of the template and disulfide bridge. A bulge in the second strand is seen at Val10, with the result that the Val10 side chain is brought onto the same face of the hairpin as that of Trp11, as seen also in Fc-III (Figure 7). A comparison with the crystal structure of bound Fc-III shows a good overlap of all backbone atoms, as well as all common side chains. In particular, the side chains of Ala3, His5, Leu6, Glu8, Val10, Trp11, and Thr13 are disposed on one face of the hairpin, whereas the disulfide bridge, Leu9, and Trp4 are on the other face, in both Fc-III and FcBP-2 (compare Figures 1 and 7).

Discussion

A key aspect of the design of peptidomimetics FcBP-1 and FcBP-2 is the use of a hairpin-stabilizing template to restrict the conformational freedom of the peptide backbone. The β-hairpin fold can then be used as a scaffold to display key residues for interaction with the surface of the Fc domain. The D-Pro-L-Pro dipeptide template is very convenient for this purpose, since the two required building blocks are commercially available and its hairpin-inducing properties have been well studied.[4−12]

The backbone β-hairpin conformation of the Fc-III peptide bound to Fc (13 residues, DCAWHLGELVWCT-NH_2) is stabilized only by a Cys-Cys disulfide bridge (Figure 1).[13] The two Cys residues occupy non-hydrogen bonding positions along the two β-strands. A type-I′ β-turn is found at the tip (Leu6-Gly7), and a β-bulge occurs at Val10 in the second β-strand in order to accommodate the noneven number of residues between the two cysteines (Cys2 and Cys12). The side chains of Asp1/Ala3/His5/Leu6/Glu8/Val10/Trp11/Thr13 are displayed on the buried face of the hairpin, whereas Trp4/Leu9 and the disulfide link cluster, on the other, solvent exposed side, in the complex with Fc (Figure 1). The side chains Val10 and Trp11 were identified by alanine substitution as energetically important groups ($\Delta\Delta G$ > 2.0 kcal/mol reduction in affinity) for binding to the Fc protein.[13]

Two Cys residues at a non-hydrogen bonding site in adjacent β-strands should represent an ideal place to insert a D-Pro-L-Pro template in the design of a synthetic β-hairpin PEM molecule (Figure 2). The resulting mimetic, FcBP-1, contains nine residues (AWHLGELVW), including the energetically important Val10 and Trp11 side chains, displayed on the β-hairpin framework. An alternative design strategy is to include four extra residues, two on each strand so as to maintain the correct geometric register of the peptide backbone. The result is mimetic FcBP-2, which now contains all 13 residues from Fc-III attached to the hairpin-stabilizing template.

In practice, these designs were only partly successful. The average solution structure of the major form of FcBP-1 shows, unexpectedly, a backbone conformation with two consecutive *cis* peptide bonds, between Trp11-^{D}Pro12 and ^{D}Pro12-^{L}Pro13 (Figures 6 and 7). The resulting distortion in the backbone conformation of the peptide loop is such that the Trp9 side chain (equivalent to Trp11 in Fc-III) now appears on the "wrong face" of the mimetic. Hence it is not surprising that FcBP-1 interacts only very weakly with the Fc domain at pH 7.4 ($IC_{50} \approx 65\mu$M in the competitive BIAcore assay (Table 1)). This structure of FcBP-1 was not expected, since ample precedence exists for the successful design of such hairpin mimetics.[4−12] However, there are many subtle influences on the conformation of the 33-membered macrocycle in FcBP-1. It is possible that the *cis*-peptide bonds, and ensuing distortion of the hairpin, arise because the required bulge at Val7 is unfavorable, or perhaps because of a preferred clustering of the hydrophobic Trp2/Leu7/Trp9 side chains on one face of the molecule (or both). The pH also has a strong influence on the conformation and Fc-binding affinity of FcBP-1. Although the precise mechanisms of these effects are not known, both conformation and affinity are clearly

related to the ionization states of amino acid side chains. A pH effect was reported[13] on the affinity of Fc-III for the Fc domain, which increases slightly from pH 7.4 to 6.0, whereas that of FcBP-1 becomes significantly worse (Table 1).

The mimicry achieved with FcBP-2, on the other hand, is excellent. The average solution structure of FcBP-2, and its similarity to the crystal structure of Fc-III, suggests that the backbone scaffold of FcBP-2 holds all the key side chains in the correct positions to interact with the Fc domain (Figures 1 and 7). The impact on affinity is seen in the direct BIAcore Fc-binding assays (Table 2), where the K_d of FcBP-2 is ~80-fold lower than that of Fc-III. However, it is the combined influence of the hairpin-inducing template coupled with a backbone cyclization and the disulfide bridge that leads to this much improved affinity. These results indicate the importance of restricting the ligand dynamics on the affinity of this ligand-Fc interaction. The affinity of the reduced form of FcBP-2 for Fc is comparable to that of Fc-III (Table 1), whereas reduction of the disulfide in Fc-III leads to a loss of activity.

This peptidomimetic-Fc interaction is a convenient system with which to explore the design, conformation, and binding properties of new turn and hairpin mimetics. For example, it would be interesting to examine whether other hairpin-inducing templates could be used instead of D-Pro-L-Pro to salvage the Fc-binding properties of the shorter mimetic FcBP-1. The new Fc-binding ligands described here may also be of value from a biotechnological viewpoint. For example, synthetic immunoglobulin-binding ligands are of interest as replacements for recombinant proteins, such as Protein-A, -G, and -L, in the affinity chromatography of therapeutic antibodies.[16] Moreover, since numerous phage display peptides against a wide variety of different proteins are now accessible,[17] the approach to synthetic ligand design exemplified here could be applied to many other medicinally and biotechnologically interesting targets.

Experimental Section

Peptide Synthesis. The peptides were synthesized by solid-phase peptide synthesis using standard Fmoc-chemistry using an Applied Biosystems 433A peptide synthesizer. The backbone-cyclic peptides were assembled on 2-chlorotrityl chloride resin (Novabiochem), while MBHA Rink amide resin (Novabiochem) was used for Fc-III. See Supporting Information.

Competition Binding Assays. The GST-Z domain fusion protein was produced in *E. coli* as follows. A DNA fragment encoding the Z domain protein was obtained by PCR using pEZZ-18 (Amersham Biosciences) as template and the following primers:

Zdomfor
5′-GCGTCCCATGGCTGCGCCGAAAGTAGACAACAAAT-3′

Zdomrev
5′-GACGACTCGAGTTAGGGTACCGAGCTCGAATTCGC-3′

The PCR product was agarose gel purified, digested with *Nco*I/*Xho*I restriction enzymes, and cloned into the vector pET42a (Novagen). The correct sequence of the product was proven by nt sequencing. GST-Z domain was produced in *E. coli* BL21(DE3)pLysS cells by growth in LB broth at 37 °C, inducing expression with 1 mM IPTG when OD_{600} = 1.1, transferring the cells to 25 °C, and harvesting the cells after 5 h (OD_{600} = 2.0). Cells were resuspended in NiNTA running buffer (Tris (20 mM), NaCl (300 mM), imidazole (20 mM), pH 7.9), lysed with a French press, and the cell lysate was applied to an NiNTA affinity column and eluted with NiNTA elution buffer (Tris (20 mM), NaCl (300 mM), imidazole (300 mM), pH 7.9). The eluted protein was dialyzed against buffer A (Tris (50 mM), EDTA (1 mM), DTT (1 mM), pH 7.5) overnight and further purified using ion-exchange chromatography (Pharmacia Mono Q 10/10 column, 2 mL/min, 0−100% NaCl (1.0 M)) in 20 column volumes). The GST-Z domain eluted as single peak at about 140 mM NaCl. The protein showed a single band by SDS-PAGE and gave a MALDI mass spectrum consistent with the expected mass. $[M + K]^+ = 39501.3 \pm 1$ *m*/*z* (calculated: 39462.6 g/mol). Expression yield: ~10 mg/L culture.

The Z domain was produced by proteolytic cleavage of the GST-Z domain with thrombin. The GST-Z domain at 1.60 mg/mL was digested with 0.4 thrombin unit/mg protein in thrombin cleavage buffer for 5−6 h at room temperature. The Z domain was purified by ion-exchange chromatography (Tris (50 mM), EDTA (1 mM), DTT (1 mM), pH 7.5; Pharmacia Mono Q 5/5 column, 1 mL/min, 0−100% NaCl (1.0 M) in 70 column volumes).

Competition BIAcore assays were carried out on a BIAcore 1000 instrument at 25 °C using HBS buffer (HEPES (10 mM), NaCl (150 mM), EDTA (3.4 mM) surfactant p20 (0.005% v/v)). The GST-Z domain was immobilized on a CM5 sensor chip by random amine coupling. The surface of the sensor chip was activated for 7 min with a solution containing 0.05 M *N*-hydroxysuccinimide (NHS)/0.2 M 3-(*N*,*N*-dimethylamino)propyl-*n*-ethylcarbodiimide (EDC) at a flow rate of 5 μL/min. The ligand at a concentration of 20 μg/mL in 10 mM acetate buffer pH 5.5 was immobilized at a density of 5950 RU on flow cell 2. A reference flow cell was prepared by immobilizing GST at a density of 5200 RU on flow cell 1. The surfaces were blocked with a 7 min injection of 1 M ethanolamine, pH 8.5. After each injection of IgG_1, the surfaces were regenerated with a 1 min pulse of 10 mM HCl. For each peptide, IC_{50} values were calculated by fitting the inhibition curves to an equation describing a one site competition binding model. The reported mean values and standard deviations derive from at least three independent experiments.

Direct Binding Assays. These measurements were performed on a BIACORE 3000 instrument at a temperature of 25 °C using HBS buffer. Human monoclonal IgG_1 (Herceptin) was immobilized on a CM5 sensor chip by random amine coupling. Surfaces were activated by injecting a solution containing 0.05 M NHS/0.2 M EDC at a flow rate of 10 μL/min for 7 min. h-IgG_1 at a concentration of 30 μg/mL in 10 mM acetate buffer pH 5.0 was immobilized at a density of 8.7 kRU and 2.7 kRU on flow cells 2 and 4, respectively. The surfaces were then blocked with a 7 min injection of 1 M ethanolamine hydrochloride pH 8.5. Two reference surfaces were prepared on flow cells 1 and 3 by immobilizing mouse anti-c-Myc monoclonal antibody (9E10) at a density of 8.0 kRU and 3.3 kRU, respectively. To collect kinetic binding data, FcBPs were each injected at seven different concentrations over the specific and reference surfaces at a flow rate of 50 μL/min for 90 s. The h-IgG_1/peptide complex was allowed to dissociate 450 s in the case of Fc-III and 900 s in the case of FcBP-2. With FcBP-2, the surfaces were regenerated at the end of the analytical cycle with a 1 min pulse of 10 mM glycine pH 3.0. With Fc-III, no regeneration step was applied. Each interaction study was repeated three times.

Biosensor data were elaborated with BIAevaluation 3.1 software. The responses from the reference surfaces 1 and 3 were subtracted from the binding responses collected over the antibody-coated surfaces 2 and 4, to correct for bulk refractive index changes. The binding data were then analyzed by nonlinear global curve fitting to a simple reversible bimolecular interaction model including the correction term for mass transport limitation. Having determined the rate constants, equilibrium dissociation constants (K_D) were calculated from the quotient k_{off}/k_{on}.

For all the interactions investigated, the data fitted well a simple 1:1 binding model. The good quality of the best-fit parameters was

(16) Roque, A. C. A.; Taipa, M. A.; Lowe, C. R. *Biotechnol. Prog.* **2004**, *20*.
(17) Sidhu, S. S. *Curr. Opin. Pharm. Biotechnol.* **2000**, *11*, 610−616.

indicated by the small and randomly distributed residuals (on average, ±2 RU) on the residual plot, the low χ^2 values (on average, <1.1 RU for flow cell 2-1, <0.5 RU for flow cell 4-3), and the small standard errors (on average, <1%) in the parameter estimates (R_{max}, k_{on}, k_{off}). The reliability of the kinetic rates was also supported by the good agreement between the kinetic rates obtained from two different surfaces.

NMR Spectroscopy. 1D and 2D ^{1}H NMR spectra of peptides were recorded at 600 MHz (Bruker DRX-600 spectrometer) or 500 MHz (Bruker AMX-500 spectrometer). Water suppression was by presaturation. Spectral assignments were based on DQF-COSY and TOCSY spectra. For NOESY, ROESY, and off-resonance ROESY spectra, a cosine window function was applied in both dimensions after zero-filling to 1024 × 2048 real points prior to Fourier transformation. Distance restraints were from NOESY or off-resonance ROESY spectra. Structure calculations were performed by restrained molecular dynamics in torsion angle space by applying the simulated annealing protocol implemented in DYANA.[18] The structure calculations started with 100 randomized conformers, and a bundle of the 20 best DYANA conformers was used for the final energy minimization procedure based on the CHARMM22 force field. The program MOLMOL[19] was used for structure analysis and visualization of the molecular models.

Acknowledgment. This work was supported by the Swiss National Science Foundation. The Functional Genomics Center Zurich is thanked for access to a BIAcore 3000 instrument.

Supporting Information Available: ^{1}H NMR assignments for peptides, tables of ROE-derived distance restraints, BIAcore sensorgrams of direct binding assays, and synthetic procedures. This material is available free of charge via the Internet at http://pubs.acs.org.

JA057513W

(18) Güntert, P.; Mumenthaler, C.; Wüthrich, K. *J. Mol. Biol.* **1997**, *273*, 283−298.
(19) Koradi, R.; Billeter, M.; Wüthrich, K. *J. Mol. Graphics* **1996**, *14*, 51−55, 29−32.